

**Photoelectron spectroscopy and ab initio calculations of small  $\text{SinSm}$  ( $n = 1,2$ ;  $m = 1-4$ ) clusters**

Xi-Ling Xu, Xiao-Jiao Deng, Hong-Guang Xu, and Wei-Jun Zheng

Citation: *The Journal of Chemical Physics* **141**, 124310 (2014); doi: 10.1063/1.4896384

View online: <http://dx.doi.org/10.1063/1.4896384>

View Table of Contents: <http://scitation.aip.org/content/aip/journal/jcp/141/12?ver=pdfcov>

Published by the [AIP Publishing](#)

---

**Articles you may be interested in**

[Negative ions of p-nitroaniline: Photodetachment, collisions, and ab initio calculations](#)

*J. Chem. Phys.* **138**, 234304 (2013); 10.1063/1.4810869

[Vibrationally resolved photoelectron imaging of platinum carbonyl anion  \$\text{Pt}\(\text{CO}\)\_n\$  \( \$n = 1-3\$ \): Experiment and theory](#)

*J. Chem. Phys.* **137**, 204302 (2012); 10.1063/1.4768004

[Ab initio calculations for the photoelectron spectra of vanadium clusters](#)

*J. Chem. Phys.* **121**, 5893 (2004); 10.1063/1.1785142

[Structure of the  \$\text{Na}\_x\text{Cl}\_{x+1}\$  \( \$x=1-4\$ \) clusters via ab initio genetic algorithm and photoelectron spectroscopy](#)

*J. Chem. Phys.* **121**, 5709 (2004); 10.1063/1.1783276

[Vibrationally resolved photoelectron spectra of  \$\text{CuCN}\$  and  \$\text{AgCN}\$  and ab initio studies of the structure and bonding in  \$\text{CuCN}\$](#)

*J. Chem. Phys.* **112**, 3627 (2000); 10.1063/1.480516

---



**AIP** | Applied Physics  
Letters

is pleased to announce **Reuben Collins**  
as its new Editor-in-Chief



# Photoelectron spectroscopy and *ab initio* calculations of small $\text{Si}_n\text{S}_m^-$ ( $n = 1,2$ ; $m = 1-4$ ) clusters

Xi-Ling Xu, Xiao-Jiao Deng, Hong-Guang Xu, and Wei-Jun Zheng<sup>a)</sup>

Beijing National Laboratory for Molecular Sciences, State Key Laboratory of Molecular Reaction Dynamics, Institute of Chemistry, Chinese Academy of Sciences, Beijing 100190, China

(Received 29 July 2014; accepted 12 September 2014; published online 26 September 2014)

Binary cluster anions composed of silicon and sulfur elements,  $\text{Si}_n\text{S}_m^-$  ( $n = 1,2$ ;  $m = 1-4$ ), were investigated by using photoelectron spectroscopy and *ab initio* calculations. The vertical detachment energies and the adiabatic detachment energies of these clusters were obtained from their photoelectron spectra. The electron affinity of SiS molecule is determined to be  $0.477 \pm 0.040$  eV. The results show that the most stable structures of the anionic and neutral  $\text{Si}_n\text{S}_m$  ( $n = 1,2$ ;  $m = 1-4$ ) clusters prefer to adopt planar configurations except that the structures of  $\text{Si}_2\text{S}_4^-$  and  $\text{Si}_2\text{S}_2$  are slightly bent.

© 2014 AIP Publishing LLC. [<http://dx.doi.org/10.1063/1.4896384>]

## I. INTRODUCTION

Silicon is one of the most abundant elements on the earth, which is very important in science and technology because of its various applications ranging from glass to catalysis to Si-based microelectronic devices.<sup>1,2</sup> Sulfur is among the ten most abundant elements in the universe, therefore, is of great astrophysical interest.<sup>3-7</sup> It is also an essential element for all life. Sulfur compounds largely exist in oil, animals, and plants.<sup>8,9</sup> The pure silicon and sulfur clusters have been extensively studied both experimentally and theoretically,<sup>10-21</sup> with investigations on their formation, stability, structures, and other physical/chemical properties. In the last decades, the molecules containing both silicon and sulfur have been the subjects of several experimental and theoretical investigations. Haas<sup>22</sup> reported the preparations, properties, structures, and chemical reactions of silicon-sulfur compounds. He suggested that the various classes of compounds, such as disilyl sulfides, silanethiols, and organothiosilanes, can be derived from the chain structure of polymeric silicon disulfide. The theoretical calculations of Davy and Holiday<sup>23</sup> have predicted the lowest energy isomer of the  $\text{SiS}_2$  cluster to be linear. Davy and Schaefer<sup>24</sup> predicted  $\text{Si}_2\text{S}$  as a singlet ring with  $C_{2v}$  symmetry by quantum-chemical calculations. Zheng and co-workers<sup>25</sup> found that silicon-sulfur cluster anions take  $\text{SiS}_2$  as the growing unit and the sulfur atoms bridge the clustering silicon atoms. Wang *et al.*<sup>26-28</sup> predicted that the clusters growing trend of  $(\text{SiS}_2)_n^\pm$  bases on the binding of the Si and S atoms, with  $\text{SiS}_2^\pm$  as the core and  $\text{SiS}_2$  as the unit. The calculations of Zwijnenburg *et al.*<sup>29</sup> suggested that the Si-S bonds in  $\text{SiS}_2$  have a considerably more covalent character than the Si-O bonds in silica.

The silicon-sulfur mixed clusters have attracted much attention also because of their astronomical interest. In 1975, Zuckerman and co-workers<sup>30</sup> reported the first detection of SiS in the envelope of the carbon star IRC+10216 with a

radio telescope of the National Radio Astronomy Observatory at Kitt Peak, Arizona. Recently, McCarthy *et al.*<sup>31</sup> measured the rotational spectrum of  $\text{Si}_2\text{S}$  by Fourier transform microwave spectroscopy (FTMS) and obtained the accurate equilibrium structural parameters for  $\text{Si}_2\text{S}$ , which provides the spectroscopic foundation for an astronomical search for  $\text{Si}_2\text{S}$ . Gauss and co-workers<sup>32</sup> determined the spectroscopic constants and equilibrium structure of cyclic  $\text{SiS}_2$  associated with FTMS and high-level calculations. Their results indicate that cyclic  $\text{SiS}_2$  is a local minimum and a plausible astronomical molecule, which may be detected with large radio telescopes in the future.

In this paper, we report a study on the electronic and geometric structures of small  $\text{Si}_n\text{S}_m^-$  ( $n = 1,2$ ;  $m = 1-4$ ) clusters with photoelectron spectroscopy and *ab initio* calculations.

## II. EXPERIMENTAL AND THEORETICAL METHODS

### A. Experimental method

The experiments were performed using a home-made apparatus consisting of a laser vaporization source, a time-of-flight (TOF) mass spectrometer, and a magnetic-bottle photoelectron spectrometer, which has been described previously.<sup>33</sup> Briefly, the  $\text{Si}_n\text{S}_m^-$  ( $n = 1,2$ ;  $m = 1-4$ ) cluster anions were produced in the laser vaporization source by laser ablation of a rotating and translating disk target (13 mm diameter, Si:S mole ratio 4:1) with the second harmonic (532 nm) light pulses from a nanosecond Nd:YAG laser (Continuum Surelite II-10). Helium gas with  $\sim 4$  atm backing pressure was allowed to expand through a pulsed valve (General Valve Series 9) into the source to cool the formed clusters. The generated cluster anions were mass-analyzed by the TOF mass spectrometer. The clusters of interest were mass-selected and decelerated before being photodetached by another laser beam. We used three types of photon energies for the photodetachment: 1064 nm and 266 nm from a Nd:YAG laser (Continuum Surelite II-10) and 193 nm (ArF) from an excimer laser. The

<sup>a)</sup> Author to whom correspondence should be addressed. Electronic mail: zhengwj@iccas.ac.cn. Tel.: +86 10 62635054. Fax: +86 10 62563167.

photodetached electrons were energy-analyzed by the magnetic-bottle photoelectron spectrometer. The photoelectron spectra were calibrated using the spectra of  $\text{Cu}^-$  and  $\text{I}^-$  taken at similar conditions. The resolution of the photoelectron spectrometer was approximately 40 meV for electrons with 1 eV kinetic energy.

## B. Theoretical method

The geometry optimizations and frequency calculations of  $\text{Si}_n\text{S}_m^-$  ( $n = 1, 2$ ;  $m = 1-4$ ) and their neutral counterparts were carried out using Density Functional Theory (DFT) with the Becke's three-parameter and Lee-Yang-Parr's gradient-corrected correlation hybrid functional (B3LYP).<sup>34,35</sup> The aug-cc-pVTZ basis set<sup>36</sup> is used for both Si and S. This theoretical method has been shown to be suitable for silicon-sulfur clusters in previous reports.<sup>29,31</sup> All the geometry optimizations were conducted without any symmetry constraint. Harmonic vibrational frequencies were calculated to make sure that the optimized structures correspond to real local minima. The single-point energies, vertical detachment energies (VDEs), and adiabatic detachment energies (ADEs) of the different isomers were also calculated by using the coupled-cluster singles and doubles augmented by a perturbative treatment of triple excitations [CCSD(T)]<sup>37</sup> method with the same basis set. The calculated energies were corrected by the zero-point vibrational energies (ZPEs) from the B3LYP calculations with the same basis set. The VDEs were calculated as the energy differences between the neutrals and the anions at the geometries of the anionic species. The ADEs were obtained as the energy differences between the neutrals and the anions with the neutral structures relaxed to the nearest local minima related to the anionic structures. All theoretical calculations in this work were performed with Gaussian 09 program package.<sup>38</sup>

## III. RESULTS AND DISCUSSION

### A. Photoelectron spectra

The photoelectron spectra of  $\text{SiS}_m^-$  ( $m = 1-4$ ) taken with 193 nm (6.424 eV) and 266 nm (4.661 eV) photons are presented in Figure 1, and those of  $\text{Si}_2\text{S}_m^-$  ( $m = 1-4$ ) are shown in Figure 2. Figure 3 shows the photoelectron spectrum of  $\text{SiS}^-$  at 1064 nm (1.165 eV). The spectra recorded with 193 nm photons show the spectral features at higher binding energy, while those at 266 nm and 1064 nm give better spectral resolution for the low electron binding energy peaks. The VDEs and the ADEs of the  $\text{Si}_n\text{S}_m^-$  ( $n = 1, 2$ ;  $m = 1-4$ ) clusters obtained from their photoelectron spectra are listed in Table I. The VDE of each cluster was taken from the maxima of the first peak in its spectrum. The ADE of each cluster was determined by adding the value of instrumental resolution to the onset of the first peak in its spectrum. The onset of the first peak was determined by drawing a straight line along the leading edge of the first peak to cross the baseline of the spectrum.

According to the spectra in Figures 1 and 2, we can see that the VDEs of the  $\text{SiS}_m^-$  and  $\text{Si}_2\text{S}_m^-$  ( $m = 1-4$ ) clusters increase with increasing number of sulfur atoms.

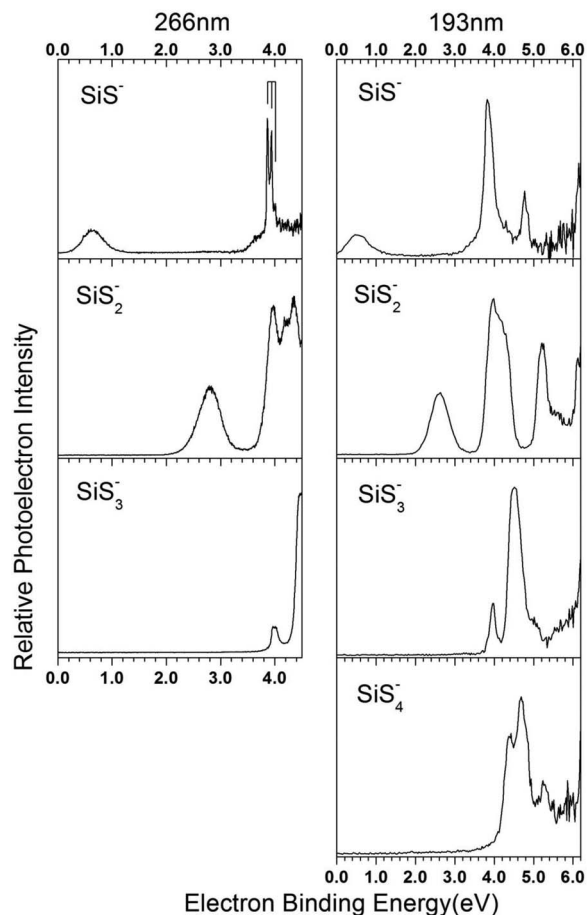


FIG. 1. Photoelectron spectra of  $\text{SiS}_m^-$  ( $m = 1-4$ ) clusters recorded with 266 nm and 193 nm photons.

### 1. $\text{SiS}_m^-$ ( $m = 1-4$ )

We measured the photoelectron spectrum of  $\text{SiS}^-$  at 193, 266, and 1064 nm. In the 193 nm spectrum of  $\text{SiS}^-$ , there are three major bands centered at 0.57, 3.87, and 4.78 eV, respectively. The second band at 3.87 eV is split into three resolved peaks centered at 3.868, 3.937, and 4.006 eV in the 266 nm spectrum. The spacing of these three peaks is approximately 0.069 eV ( $557 \text{ cm}^{-1}$ ), which corresponds to the vibrational frequency of the first electronic excited state of  $\text{SiS}$  ( $^3\Pi_1$ ). In the 1064 nm spectrum of  $\text{SiS}^-$ , five resolved peaks are observed, which correspond to the first band of the spectra taken with 193 and 266 nm. The five sharp peaks centered at 0.477, 0.566, 0.657, 0.758, 0.865 eV can be tentatively assigned to the vibrational progression related to the transition from the ground state of  $\text{SiS}^-$  to the electronic ground state ( $^1\Sigma^+$ ) of  $\text{SiS}$  neutral. The separation of the vibrational progression is about 0.097 eV ( $780 \text{ cm}^{-1}$ ), which is in agreement with the vibrational frequency ( $\omega_e = 749.6 \text{ cm}^{-1}$ ) of  $\text{SiS}$  ( $^1\Sigma^+$ ) reported by Harris *et al.*<sup>39</sup>

Four major bands centered at 2.64, 4.10, 5.23, and 6.12 eV are observed in the spectrum of  $\text{SiS}_2^-$  at 193 nm. The first band is determined more precisely to be 2.79 eV in the 266 nm spectrum. The second band at 4.10 eV is split into two resolved peaks centered at 3.96 and 4.34 eV at 266 nm. In the spectrum of  $\text{SiS}_3^-$ , we are able to distinguish two bands

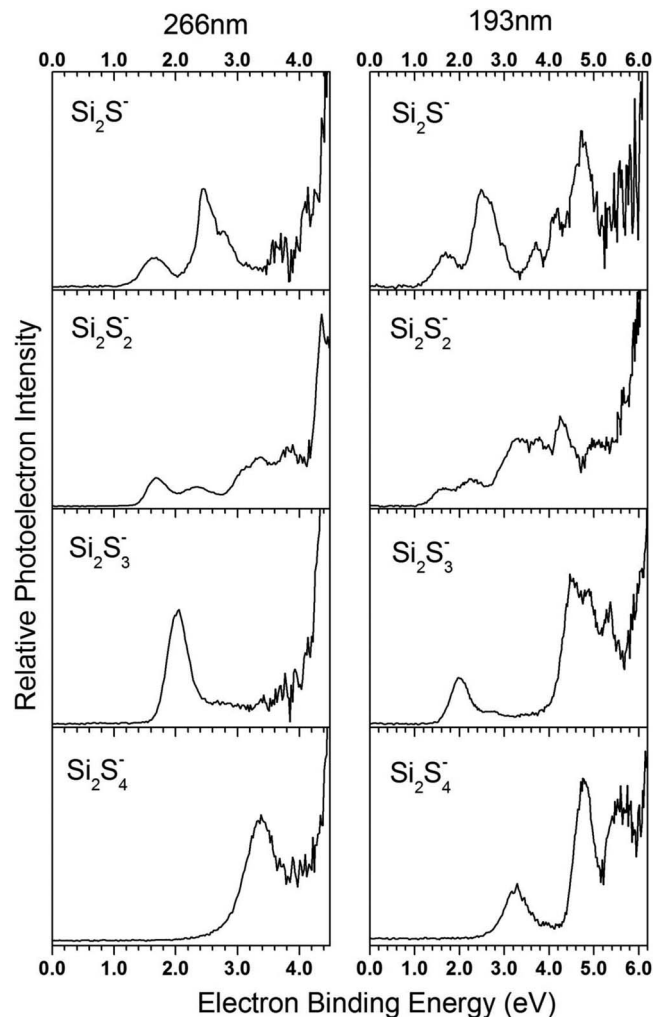


FIG. 2. Photoelectron spectra of  $\text{Si}_2\text{S}_m^-$  ( $m = 1-4$ ) clusters recorded with 266 nm and 193 nm photons.

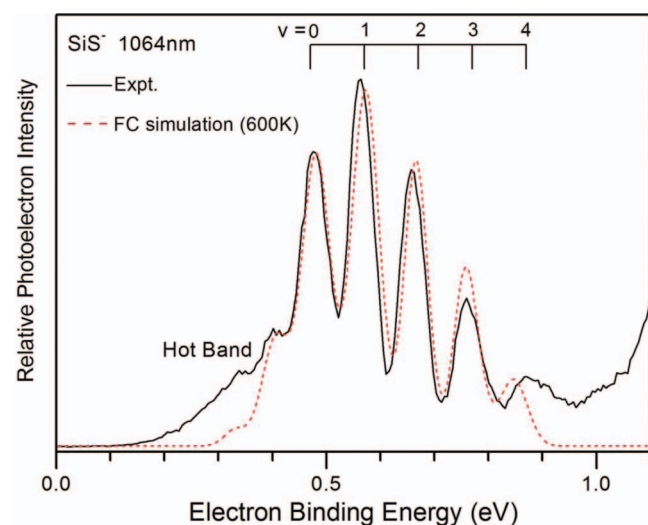


FIG. 3. Photoelectron spectrum of  $\text{SiS}^-$  cluster recorded with 1064 nm photons. The solid line stands for the experimental data. The red dashed line comes from the Franck-Condon simulation. The temperature of  $\text{SiS}^-$  cluster is set at 600 K. The geometries and vibration frequencies of anion  $\text{SiS}^-$  and neutral  $\text{SiS}$  calculated at B3LYP/aug-cc-pVTZ level are utilized in FC simulation.

TABLE I. Experimental VDEs and ADEs of  $\text{Si}_n\text{S}_m^-$  ( $n = 1,2; m = 1-4$ ) clusters estimated from their photoelectron spectra.<sup>a</sup>

Cluster	VDE (eV)	ADE (eV)
$\text{SiS}^-$	$0.566 \pm 0.040$	$0.477 \pm 0.040$
$\text{SiS}_2^-$	$2.79 \pm 0.08$	$2.34 \pm 0.08$
$\text{SiS}_3^-$	$4.00 \pm 0.08$	$3.92 \pm 0.08$
$\text{SiS}_4^-$	$4.39 \pm 0.08$	$4.08 \pm 0.08$
$\text{Si}_2\text{S}^-$	$1.65 \pm 0.08$	$1.37 \pm 0.08$
$\text{Si}_2\text{S}_2^-$	$1.68 \pm 0.08$	$1.50 \pm 0.08$
$\text{Si}_2\text{S}_3^-$	$2.02 \pm 0.08$	$1.76 \pm 0.08$
$\text{Si}_2\text{S}_4^-$	$3.36 \pm 0.08$	$2.84 \pm 0.08$

<sup>a</sup>The VDE and ADE of  $\text{SiS}^-$  are estimated from its 1064 nm photoelectron spectrum. The VDE and ADE of  $\text{SiS}_4^-$  are estimated from its 193 nm photoelectron spectrum. Those of the others  $\text{Si}_n\text{S}_m^-$  clusters are estimated from their 266 nm photoelectron spectra.

centered at 4.00 and 4.51 eV. Due to the higher electron binding energy of  $\text{SiS}_4^-$ , only the 193 nm photoelectron spectrum for  $\text{SiS}_4^-$  was taken. As shown in Figure 1, the photoelectron spectrum of  $\text{SiS}_4^-$  has three resolved peaks centered at 4.39, 4.68, and 5.26 eV, respectively.

## 2. $\text{Si}_2\text{S}_m^-$ ( $m = 1-4$ )

The spectrum of  $\text{Si}_2\text{S}^-$  at 193 nm has five features centered at 1.65, 2.58, 3.70, 4.16, and 4.73 eV, respectively. The second feature at 2.58 eV is split into two peaks centered at 2.45 and 2.78 eV in the 266 nm spectrum. There are more than five bands in the  $\text{Si}_2\text{S}_2^-$  spectrum at 193 nm, and the first two bands centered at 1.68 and 2.31 eV are weaker than the others. The spectrum of  $\text{Si}_2\text{S}_3^-$  at 193 nm contains two major bands, in which one centered at 2.02 eV is clearly resolved and another higher energy band has three barely resolved peaks centered at 4.53, 4.88, and 5.53 eV, respectively. The spectrum of  $\text{Si}_2\text{S}_4^-$  at 193 nm exhibits three bands centered at 3.27, 4.79, and 5.62 eV, respectively. The first band is determined more precisely to be 3.36 eV in the 266 nm spectrum.

## B. Theoretical results

The optimized geometries of the low-lying isomers of the  $\text{Si}_n\text{S}_m^-$  ( $n = 1,2; m = 1-4$ ) clusters are presented in Figure 4 with the most stable structures on the left. Figure 5 displayed the optimized geometries of the low-lying isomers of the neutral  $\text{Si}_n\text{S}_m$  ( $n = 1,2; m = 1-4$ ) clusters with the most stable structures on the left. We have considered many different initial structures and multiplicities in the calculations. The Cartesian coordinates of the low-lying isomers of  $\text{Si}_n\text{S}_m^-$  ( $n = 1,2; m = 1-4$ ) are available in the supplementary material.<sup>40</sup>

The symmetries, relative energies, and theoretical VDEs and ADEs of these low-lying anionic isomers are summarized in Table II along with the experimental VDEs and ADEs for comparison. The VDEs of the most stable isomers calculated with the CCSD(T) method are in excellent agreement with the experimental values. The harmonic vibrational frequencies as well as the infrared intensities, dipole moments, and rotational constants of the most stable  $\text{Si}_n\text{S}_m$  neutral clusters at the B3LYP/aug-cc-pVTZ level are available in the

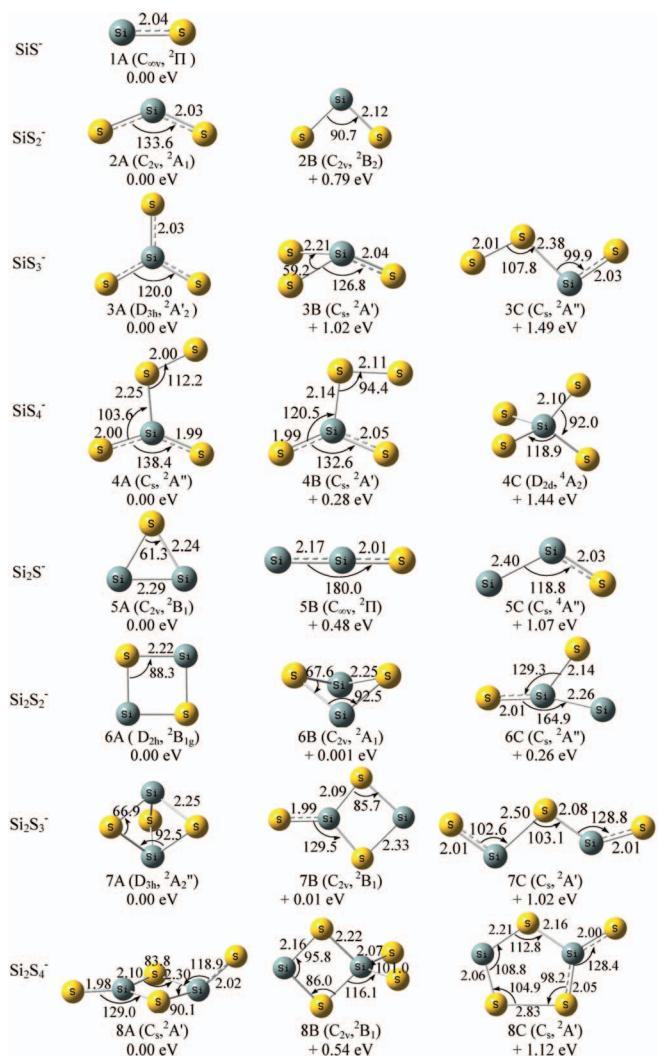


FIG. 4. Geometries of the low-lying isomers of  $\text{Si}_n\text{S}_m^-$  ( $n = 1, 2; m = 1-4$ ) clusters optimized at B3LYP/aug-cc-pVTZ level. The energies relative to the most stable isomers are obtained by using the CCSD(T) method. Bond lengths (in angstrom) and bond angles (in degree) are also shown.

supplementary material.<sup>40</sup> We have also simulated the photoelectron spectra of different isomers based on theoretically generalized Koopmans' theorem (GKT)<sup>41,42</sup> and compared the simulated spectra with the experimental results in Figure 6. For convenience, we call the simulated spectra as density of states (DOS) spectra.<sup>42</sup> Each transition, as the vertical lines in the DOS spectra, corresponds to the removal of an electron from a specific molecular orbital of the cluster anion. In the simulation, the first peak associated with the HOMO was set at the position of theoretical VDE, and the other peaks associated with the deeper orbitals were shifted to higher binding energies side according to the relative energies of orbitals ( $\Delta E_n$ ). The values of  $\Delta E_n$  were calculated by the equation:  $\Delta E_n = E_{(\text{HOMO})} - E_{(\text{HOMO}-n)}$ , where  $E_{(\text{HOMO})}$  is the energy of the HOMO,  $E_{(\text{HOMO}-n)}$  is the energy of the HOMO-n orbital from theoretical calculations. The peak associated with each orbital was fitted with a unit-area Gaussian function of 0.2 eV full width at half maximum (FWHM). It should be noted that the theoretical VDEs discussed in the following paragraphs are from the CCSD(T) calculations and

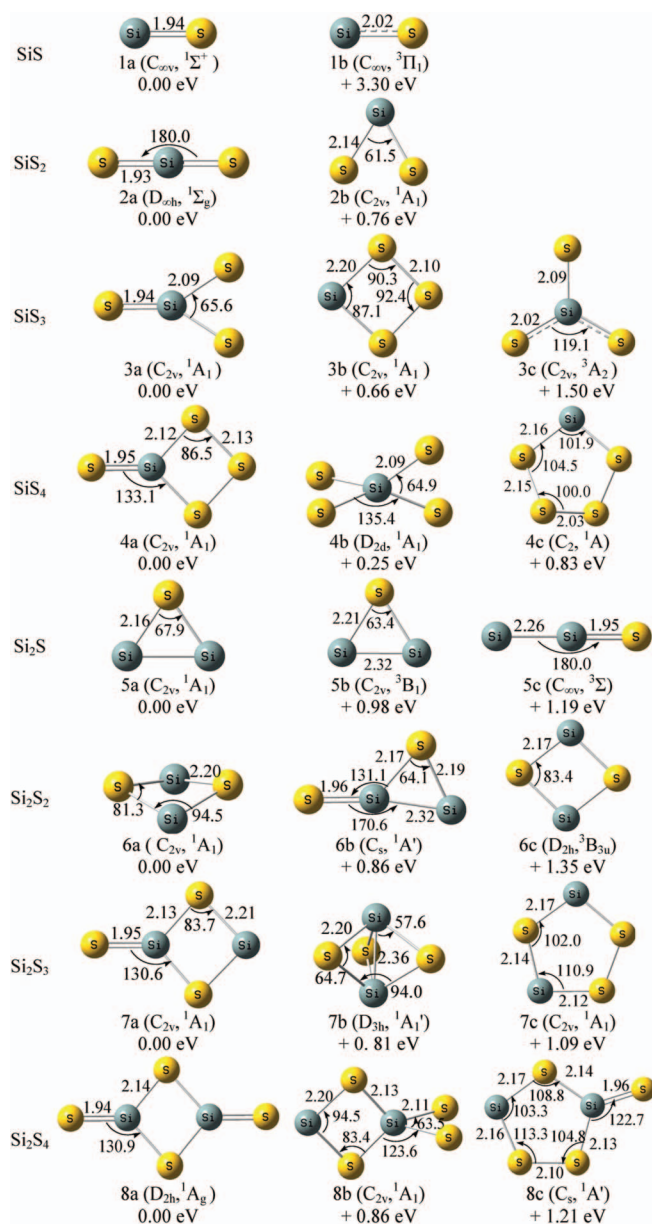


FIG. 5. Geometries of the low-lying isomers of  $\text{Si}_n\text{S}_m$  ( $n = 1, 2; m = 1-4$ ) clusters optimized at B3LYP/aug-cc-pVTZ level. The energies relative to the most stable isomers are obtained by using the CCSD(T) method. Bond lengths (in angstrom) and bond angles (in degree) are also shown.

the DOS spectra of  $\text{Si}_n\text{S}_m^-$  ( $n = 1, 2; m = 1-4$ ) are produced at the CCSD(T) /aug-cc-pVTZ level.

### 1. Structures of $\text{SiS}_m^-$ and $\text{SiS}_m$ ( $m = 1-4$ )

*a. SiS<sup>-</sup> and SiS.*  $\text{SiS}^-$  is of  $C_{\infty v}$  symmetry with a  $^2\Pi$  electronic state. The calculated Si-S bond length of  $\text{SiS}^-$  is 2.04 Å. The theoretical VDE (0.60 eV) of  $\text{SiS}^-$  is in good agreement with the experimental value (0.566 eV). In Figure 6, the DOS spectrum of 1A is also very similar to the experimental spectrum of  $\text{SiS}^-$ . For the ground state of the neutral SiS (1a), our calculations show that the Si-S bond length is 1.94 Å, shorter than that of the anion by 0.10 Å. The Si-S bond of SiS is longer than the calculated Si-O bond (1.54 Å) of its isoelectronic SiO molecule by  $\sim 0.40$  Å.<sup>43</sup> The calculated vibrational

TABLE II. Relative energies, theoretical VDEs and ADEs of the low-lying isomers of  $\text{Si}_n\text{S}_m^-$  ( $n = 1, 2; m = 1-4$ ) clusters, as well as the experimental VDEs and ADEs estimated from their photoelectron spectra. The isomers labeled in bold are the most probable isomers in the experiments.

Isomer	State	Sym.	$\Delta E^a$ (eV)	VDE (eV)			ADE (eV)			
				Theo.		Expt.	Theo.		Expt.	
				B3LYP	CCSD(T)		B3LYP	CCSD(T)		
$\text{SiS}^-$	<b>1A</b>	$^2\Pi$	$C_{\infty v}$	0.00	0.76	0.60	0.566	0.64	0.50	0.477
$\text{SiS}_2^-$	<b>2A</b>	$^2A_1$	$C_{2v}$	0.00	2.82	2.67	2.79	1.95	1.81	2.34
	2B	$^2B_2$	$C_{2v}$	0.79	3.07	3.10		2.01	1.80	
$\text{SiS}_3^-$	<b>3A</b>	$^2A_2'$	$D_{3h}$	0.00	4.43	4.02	4.00	3.28	2.92	3.92
	3B	$^2A'$	$C_s$	1.02	3.08	2.95		2.03	1.90	
	3C	$^2A''$	$C_s$	1.49	3.17	3.35		3.01	2.98	
$\text{SiS}_4^-$	<b>4A</b>	$^2A''$	$C_s$	0.00	4.19	4.51	4.39	3.84	3.92	4.08
	4B	$^2A'$	$C_s$	0.28	3.69	3.79		2.61	2.37	
	4C	$^4A_2$	$D_{2d}$	1.44	4.31	3.94		2.68	2.50	
$\text{Si}_2\text{S}^-$	<b>5A</b>	$^2B_1$	$C_{2v}$	0.00	1.74	1.65	1.65	1.56	1.48	1.37
	5B	$^2\Pi$	$C_{\infty v}$	0.48	2.25	2.29		2.16	2.20	
	5C	$^4A''$	$C_s$	1.07	2.07	2.16		1.57	1.59	
$\text{Si}_2\text{S}_2^-$	<b>6A</b>	$^2B_{1g}$	$D_{2h}$	0.00	1.74	1.64	1.68	1.63	1.52	1.50
	<b>6B</b>	$^2A_1$	$C_{2v}$	0.001	2.29	2.22		1.55	1.52	
	6C	$^2A''$	$C_s$	0.26	2.41	2.33		2.19	2.12	
$\text{Si}_2\text{S}_3^-$	<b>7A</b>	$^2A_2''$	$D_{3h}$	0.00	2.93	2.78		2.81	2.65	
	<b>7B</b>	$^2B_1$	$C_{2v}$	0.01	2.11	2.07	2.02	1.91	1.82	1.76
	7C	$^2A'$	$C_s$	1.02	3.54	3.98		2.69	2.59	
$\text{Si}_2\text{S}_4^-$	<b>8A</b>	$^2A'$	$C_s$	0.00	3.44	3.34	3.36	2.38	2.24	2.84
	8B	$^2B_1$	$C_{2v}$	0.54	4.17	4.09		2.79	2.56	
	8C	$^2A'$	$C_s$	1.12	3.79	3.67		2.52	2.33	

<sup>a</sup>The  $\Delta E$  values are from the CCSD(T) method.

frequency of  $\text{SiS}$  (1a) is  $741\text{ cm}^{-1}$ , which is in agreement with the vibrational spacing ( $780\text{ cm}^{-1}$ ) observed experimentally in this work (Figure 3) and the result ( $749.6\text{ cm}^{-1}$ ) reported by Harris *et al.*<sup>39</sup> We find an electronic excited state of the neutral  $\text{SiS}$  (2b), which is higher than the ground state of  $\text{SiS}$  by 3.30 eV in energy (Figure 5). The calculated results in Table II and Figure 5 indicate that the energies of  $\text{SiS } ^1\Sigma^+$  and  $\text{SiS } ^3\Pi_1$  relative to the ground state of  $\text{SiS}^- (^2\Pi)$  are 0.50 and 3.80 eV, respectively. They are consistent with the positions of the first two bands in the spectra of 193 and 266 nm. The calculated vibrational frequency of the excited state ( $\text{SiS } ^3\Pi_1$ ) is  $583\text{ cm}^{-1}$ , which is in agreement with the separation ( $557\text{ cm}^{-1}$ ) of the second band in the range of 3.80-4.20 eV in the 266 nm spectrum of  $\text{SiS}^-$ . It should be noted that the second band of  $\text{SiS}^-$  in the range of 3.45-4.20 eV at 266 nm also includes several electronic excited states and the rising edge (3.45-3.80 eV) of the band may be attributed to the hot bands, similar to the hot bands in the spectrum of 1064 nm.

In order to verify the assignment of the vibrational progression in the 1064 nm spectrum, Franck-Condon (FC) simulation was performed by using the ezSpectrum program<sup>44</sup> to assure the  $0\leftarrow 0$  band of  $\text{SiS} (X^1\Sigma^+) \leftarrow \text{SiS}^- (X^2\Pi)$  transition using the frequencies and geometries of  $\text{SiS} (X^1\Sigma^+)$  and  $\text{SiS}^- (X^2\Pi)$  calculated at B3LYP/aug-cc-pVTZ level (Figure 3). In the spectrum simulation, a FWHM of  $440\text{ cm}^{-1}$  was utilized with Gaussian band envelopes. The red dashed line in Figure 3 is the simulation result by setting the temperature of the  $\text{SiS}^-$  anion at 600 K, which is in good agreement with

the experiment data with slightly difference for the onset. The position of  $0\leftarrow 0$  transition, which stands for the adiabatic detachment energy of  $\text{SiS}^-$  or the electron affinity of the neutral  $\text{SiS}$ , is determined to be  $0.477 \pm 0.040\text{ eV}$  and corresponds to the transition from the vibrational ground state of  $\text{SiS}^-$  to that of the neutral  $\text{SiS}$ . The second peak, which stands for the vertical detachment energy of  $\text{SiS}^-$ , is determined to be  $0.566 \pm 0.040\text{ eV}$ . The hot bands are slightly serious in the experimental spectrum. The probable reason is that the  $\text{SiS}^-$  cluster is hot in our experiments due to its small size. This is confirmed by the FC simulation as the temperature of the anion is about 600 K in the FC simulation. Note that the temperature of the  $\text{SiS}^-$  was high because it is of small size and had experienced few collisions in the molecular beam while the temperatures of the larger  $\text{Si}_n\text{S}_m^-$  clusters were lower because they had experienced more collisions in the molecular beam.

*b.  $\text{SiS}_2^-$  and  $\text{SiS}_2$ .* We have found two low-lying isomers for  $\text{SiS}_2^-$ , which are both S-Si-S bent structures with  $C_{2v}$  symmetry in different electronic states. The Si-S bond length of isomer 2A is 2.03 Å. The  $\angle\text{SSiS}$  bond angle of isomer 2A in  $^2A_1$  electronic state is  $133.6^\circ$ , similar to the  $\angle\text{OSiO}$  bond angle ( $140^\circ$ ) of its isoelectronic  $\text{SiO}_2^-$  anion.<sup>45</sup> The  $\angle\text{SSiS}$  bond angle of isomer 2B is about  $90.7^\circ$ , similar to the stable structure of  $\text{SiS}_2^-$  reported by Wang *et al.*<sup>27</sup> In our work, the energy of isomer 2B is higher than that of isomer 2A by 0.79 eV, and the predicted VDE (3.10 eV) of isomer 2B is much higher than the experimental value (2.79 eV). The

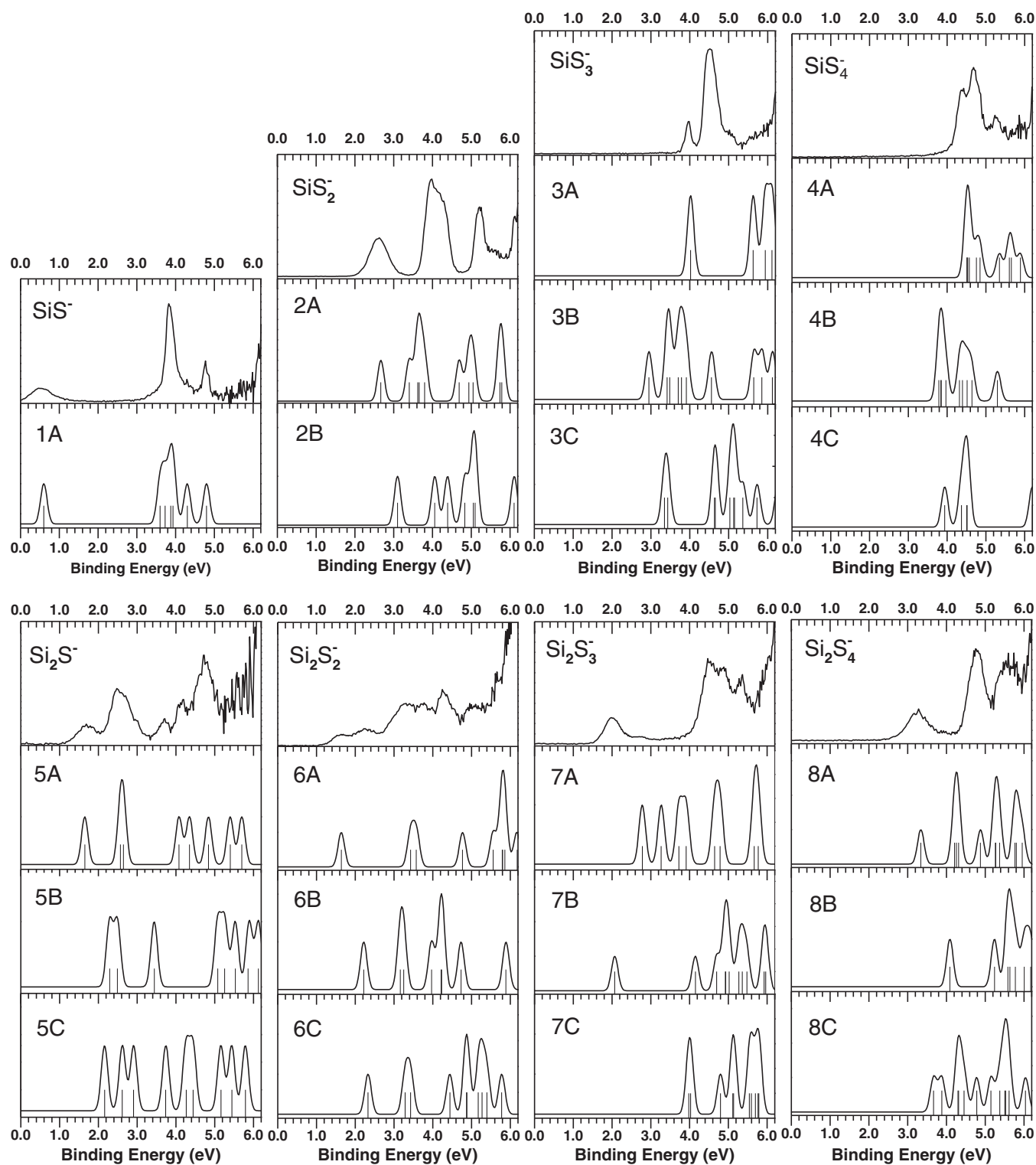


FIG. 6. Comparison of the experimental photoelectron spectra of  $\text{Si}_n\text{S}_m^-$  ( $n = 1, 2; m = 1-4$ ) clusters with their simulated DOS spectra at CCSD(T)/aug-cc-pVTZ level. The simulations were conducted by fitting the distribution of the transition lines with unit-area Gaussian functions of 0.2 eV full width at half maximum. The vertical lines are the theoretical simulated spectral lines of  $\text{Si}_n\text{S}_m^-$  ( $n = 1, 2; m = 1-4$ ) clusters.

calculated VDE of isomer 2A is 2.67 eV, in excellent agreement with the experimental measurement. In Figure 6, the simulated DOS spectrum of isomer 2A also agrees with the experimental spectrum. Therefore, we can infer that isomer 2A is the most likely structure of  $\text{Si}_2\text{S}_2^-$  in our experiments. Although isomer 2B is a real minimum on the  $\text{Si}_2\text{S}_2^-$

potential energy surface, it cannot exist in our experiments due to its high energy. For the neutral  $\text{Si}_2\text{S}_2$ , the most stable isomer 2a is a S-Si-S linear structure with  $D_{\infty h}$  symmetry, similar to  $\text{CS}_2$  and  $\text{SiO}_2$ , and consistent with Walsh rule's<sup>32,46</sup> as well as the result obtained by Davy and Holiday.<sup>23</sup> Its Si-Si bond length is 1.93 Å, which is shorter than that of isomer 2A.

For isomer 2b, the  $\angle\text{SSiS}$  angle is  $61.5^\circ$ , smaller than those of isomers 2A and 2B.

*c.  $\text{SiS}_3^-$  and  $\text{SiS}_3$ .* We obtained three low-lying isomers for  $\text{SiS}_3^-$ . The most stable structure of  $\text{SiS}_3^-$  (3A) is of  $D_{3h}$  symmetry without any S–S bond and the Si–S bond length is 2.03 Å. Isomer 3B is a non-planar  $C_s$  structure without any S–S bond. Isomer 3C is a *trans*-planar structure of  $C_s$  symmetry. The theoretical VDE (4.02 eV) of isomer 3A is in good agreement with the experimental measurement (4.00 eV). The energies of isomers 3B and 3C are 1.02 eV and 1.49 eV higher than that of isomer 3A, respectively. The simulated DOS spectrum of isomer 3A is in better agreement with the experimental spectrum than those of isomers 3B and 3C. Then, we suggest that isomer 3A is the most likely structure for  $\text{SiS}_3^-$ . For the neutral  $\text{SiS}_3$ , the most stable isomer 3a is a Y-shaped structure with  $C_{2v}$  symmetry. There are two kinds of Si–S bonds and the bond lengths are 1.94 and 2.09 Å, respectively. Isomer 3b is a four-membered ring structure of  $C_{2v}$  symmetry. Isomer 3c with  $C_{2v}$  symmetry is similar to the structure of isomer 3A.

*d.  $\text{SiS}_4^-$  and  $\text{SiS}_4$ .* For  $\text{SiS}_4^-$ , the most stable isomer (4A) has  $C_s$  symmetry. The fourth sulfur atom attaches to one of three sulfur atoms of  $\text{SiS}_3^-$ . The structure of isomer 4B is similar to that of isomer 4A with slightly difference in  $\angle\text{SSSi}$  angle. Isomer 4C is a 3D structure with two  $\text{SiS}_2$  subunits perpendicular to each other. The calculated VDE of isomer 4A is 4.51 eV, which is consistent with the experimental value (4.39 eV). The energies of isomers 4B and 4C are 0.28 eV and 1.44 eV higher than that of isomer 4A, respectively, and their theoretical VDEs are different from the experimental measurement. The simulated DOS spectrum of isomer 4A is also consistent with the experimental spectrum. Therefore, isomer 4A is what we observed in our experiments. For  $\text{SiS}_4$  neutral, isomer 4a has a four-membered ring  $\text{SiS}_3$  and with an additional S atom attaching to the Si atom. Isomer 4b is a 3D configuration with  $D_{2d}$  symmetry, which is similar to isomer 4C. Isomer 4c is a distorted five-membered ring structure with  $C_2$  symmetry.

## 2. Structures of $\text{Si}_2\text{S}_m^-$ and $\text{Si}_2\text{S}_m$ ( $m = 1-4$ )

*a.  $\text{Si}_2\text{S}^-$  and  $\text{Si}_2\text{S}$ .* For  $\text{Si}_2\text{S}^-$ , the most stable isomer (5A) is an isosceles triangle structure with  $C_{2v}$  symmetry. The Si–S bond length of isomer 5A is 2.24 Å, longer than that of  $\text{SiS}_2^-$  (2.03 Å), and the  $\angle\text{SiSSi}$  angle is  $61.3^\circ$ . Isomer 5B is a Si–Si–S linear structure with  $C_{\infty v}$  symmetry and isomer 5C is a Si–Si–S bent structure. The calculated VDE (1.65 eV) of isomer 5A is in excellent agreement with the experimental value (1.65 eV). The simulated DOS spectrum of isomer 5A is also in good agreement with the experimental spectrum of  $\text{Si}_2\text{S}^-$ . The VDEs of isomers 5B and 5C deviate from our experimental result. And the energies of isomers 5B and 5C are much higher than that of isomer 5A. Therefore, the existence of isomers 5B and 5C in our experiments can be ruled out. Isomer 5A is the most probable one detected in our experiments. For the neutral  $\text{Si}_2\text{S}$ , the most stable isomer (5a) is an isosceles triangle structure in  $^1A_1$  state, consistent with the predicted structure by Davy and Schaefer.<sup>24</sup> The Si–S bond length of

isomer 5a is 2.16 Å, shorter than that of isomer 5A, and the  $\angle\text{SiSSi}$  angle is  $67.9^\circ$ . Isomer 5b is also an isosceles triangle structure in  $^3B_1$  electronic state. The Si–S bond length of isomer 5b is 2.21 Å, slightly shorter than that of isomer 5A, and the  $\angle\text{SiSSi}$  angle is  $63.4^\circ$ . The structure of isomer 5c is linear (Si–Si–S) with  $C_{\infty v}$  symmetry.

*b.  $\text{Si}_2\text{S}_2^-$  and  $\text{Si}_2\text{S}_2$ .* The first two isomers of  $\text{Si}_2\text{S}_2^-$  are nearly degenerate in energy, with isomer 6B higher than isomer 6A by only 0.001 eV. Isomer 6A is a rhombus structure with alternating Si–S bonds, and has  $D_{2h}$  symmetry with a  $^2B_{1g}$  electronic state. The Si–S bond length of isomer 6A is 2.22 Å. Isomer 6B is a non-planar four-membered ring (dihedral angle of S–SiSi–S is about  $121^\circ$ ) of  $C_{2v}$  symmetry. The calculated VDE (1.64 eV) of isomer 6A is in good agreement with the experimental measurement (1.68 eV). The theoretical VDE of isomer 6B is calculated to be 2.22 eV, much higher than that of the first peak (1.68 eV) in the experimental spectrum of  $\text{Si}_2\text{S}_2^-$ , but fits the feature in the range of 1.92–2.60 eV very well. The energy of isomer 6C is higher than that of isomer 6A by 0.26 eV and its theoretical VDE is very different from our experimental result. As we can see in Figure 6, the simulated DOS spectrum of isomer 6A may contribute to a part of photoelectron features and that of isomer 6B agrees well with other part in the experimental spectrum of  $\text{Si}_2\text{S}_2^-$ . The combination of the DOS spectra of isomers 6A and 6B can fit the experimental spectrum very well. As a result, we suggest that isomers 6A and 6B coexist in our experiments. For  $\text{Si}_2\text{S}_2$  neutral, the structure of isomer 6a is a non-planar four-membered ring (dihedral angle of S–SiSi–S is about  $151^\circ$ ) with a  $^1A_1$  electronic state. It is the only non-planar structure among the most stable isomers of  $\text{Si}_n\text{S}_m$  ( $n = 1, 2$ ;  $m = 1-4$ ) neutrals. The slightly folding of the  $\text{Si}_2\text{S}_2$  rhombus probably is due to repulsion of the Si–S bonds by the non-bonding valent electrons of the Si atoms. Isomer 6b is a planar structure, which consists of a three-membered ring  $\text{Si}_2\text{S}$  and a Si=S double bond. Isomer 6c is a rhombus  $D_{2h}$  structure.

*c.  $\text{Si}_2\text{S}_3^-$  and  $\text{Si}_2\text{S}_3$ .* We displayed three low-lying isomers for  $\text{Si}_2\text{S}_3^-$ . Isomer 7A is a  $D_{3h}$  symmetric trigonal bipyramid with the two silicon atoms capping on the opposite sides of the plane formed by the three sulfur atoms. Isomer 7B is a planar structure with  $C_{2v}$  symmetry, has a  $\text{Si}_2\text{S}_2$  four-membered ring and the third S atom attaching to one of the Si atoms in the  $\text{Si}_2\text{S}_2$  ring. Isomer 7B lies only 0.01 eV above isomer 7A. Isomer 7C is a W-shaped structure with alternating S–Si bonds. The energy of isomer 7C is higher than that of isomer 7A by 1.02 eV, and its theoretical VDE (3.98 eV) is very different from our experimental result (2.02 eV). The calculated VDE of isomer 7B is 2.07 eV, in excellent agreement with the experimental measurement. In Figure 6, we can see that the simulated DOS spectrum of isomer 7B fits well with the experimental spectrum of  $\text{Si}_2\text{S}_3^-$ . Although the theoretical VDE (2.78 eV) of isomer 7A is different from the experimental value, its DOS spectrum may contribute to some of the signals in the range of 2.60–4.00 eV in the experimental spectrum. Thus, we suggest that isomer 7B is the dominant structure in our experiments, and isomer 7A may contribute to



some of the low intensity peaks in the experimental spectra. For the neutral  $\text{Si}_2\text{S}_3$ , the most stable structure (isomer 7a) is similar to isomer 7B of the anion, and the second stable structure (isomer 7b) is similar to isomer 7A of the anion. Isomer 7c is a five-membered ring with  $C_{2v}$  symmetry. As we can see in Figure 5, the trigonal bipyramid structure (7b) is much less stable than the planar structure (7a). Since isomer 7a is much more stable than the other isomers, it may have a larger population in our cluster source. And it is easy for isomer 7a of the  $\text{Si}_2\text{S}_3$  neutral to get an electron to form isomer 7B of the  $\text{Si}_2\text{S}_3^-$  anion. This probably can explain why isomer 7B is the dominant isomer of the anion that contributed to the experimental spectrum of  $\text{Si}_2\text{S}_3^-$ .

*d.  $\text{Si}_2\text{S}_4^-$  and  $\text{Si}_2\text{S}_4$ .* We obtained three low-lying isomers for  $\text{Si}_2\text{S}_4^-$ . Isomer 8A has  $C_s$  symmetry. It is the only non-planar structure among the most stable isomers of  $\text{Si}_n\text{S}_m^-$  ( $n = 1, 2; m = 1-4$ ). It can be viewed as two S atoms attaching to a  $\text{Si}_2\text{S}_2$  four-membered ring. It has two bridging S atoms and two terminal S atoms. One of the terminal S atoms is bent out of the plane due to the repulsion from the negative charge, similar to the case of  $\text{Si}_2\text{O}_4^-$ .<sup>45</sup> Isomer 8B has  $C_{2v}$  symmetry with a  $\text{Si}_2\text{S}_2$  rhombus and a  $\text{SiS}_2$  subunit perpendicular to the plane of the  $\text{Si}_2\text{S}_2$  rhombus, which is similar to the most stable structure of  $\text{Si}_2\text{S}_4^-$  calculated by Wang *et al.*<sup>27</sup> However, we found that isomer 8A is the most stable structure of  $\text{Si}_2\text{S}_4^-$  rather than isomer 8B. Isomer 8C has  $C_s$  symmetry with a five-membered ring  $\text{Si}_2\text{S}_3$  and a terminal Si-S bond. The theoretical VDE of isomer 8A is 3.34 eV, which is consistent with the experimental value (3.36 eV). The energies of isomers 8B and 8C are both much higher than that of isomer 8A, and their calculated VDEs deviate from our experimental result. In Figure 6, the simulated DOS spectrum of isomer 8A is much more similar to the observed spectrum of  $\text{Si}_2\text{S}_4^-$  than those of isomers 8B and 8C. Therefore, the existence of isomers 8B and 8C in our experiments can be ruled out. Isomer 8A is the most probable one detected in our experiments. For the neutral  $\text{Si}_2\text{S}_4$ , its ground state structure (8a) has a  $D_{2h}$  planar structure with a  $\text{Si}_2\text{S}_2$  rhombus and two terminal Si=S double bonds, which is in agreement with the calculated result by Wang *et al.*<sup>28</sup> The structure of isomer 8b is similar to that of isomer 8B, which includes a  $\text{Si}_2\text{S}_2$  rhombus and a  $\text{SiS}_2$  subunit perpendicular to the plane of the rhombus. The structure of isomer 8c is planar with a five-membered ring and a terminal Si=S double bond.

In summary, the most stable isomers of the anionic  $\text{Si}_n\text{S}_m^-$  ( $n = 1, 2; m = 1-4$ ) clusters are all planar structures except for  $\text{Si}_2\text{S}_4^-$ . The most stable structures of the neutral  $\text{Si}_n\text{S}_m$  ( $n = 1, 2; m = 1-4$ ) clusters are all planar with the exception of  $\text{Si}_2\text{S}_2$ . As we can see from Figure 4, the most stable isomers of  $\text{SiS}_m^-$  ( $m = 1-4$ ) can be obtained by binding one S atom to the Si atom of the most stable isomers of  $\text{SiS}_{m-1}^-$  with the exception of  $\text{SiS}_4^-$ , whose structure is the fourth S atom attaches to one of the three S atoms of  $\text{SiS}_3^-$ . For  $\text{Si}_2\text{S}_m^-$  ( $m = 1-4$ ), the most stable structures can be derived by attaching one S atom to one of the Si atoms of the most stable structure of  $\text{Si}_2\text{S}_{m-1}^-$ . For the neutral  $\text{Si}_n\text{S}_m$  ( $n = 1, 2; m = 1-4$ ) clusters, their most stable isomers are all much lower in energy than the other isomers (Figure 5). The comparison

of the structures of anionic and neutral  $\text{Si}_n\text{S}_m$  clusters indicates that the structures are charge dependent, and the broad features observed in our experiments also indicate that there is a significant geometry change between the anions and the neutrals, therefore, the experimental ADEs of  $\text{Si}_n\text{S}_m^-$  anions cannot be simply considered as the electron affinities (EAs) of  $\text{Si}_n\text{S}_m$  neutrals.

It would be interesting to compare the structures of  $\text{Si}_n\text{S}_m$  ( $n = 1, 2; m = 1-4$ ) clusters with their isoelectronic counterparts such as  $\text{Si}_n\text{O}_m$  and  $\text{C}_n\text{S}_m$  clusters which were investigated previously by a number of experiments and theoretical calculations.<sup>43,45,47-57</sup> The earlier theoretical calculations<sup>49</sup> suggested that the lowest-energy structures of the neutral  $\text{Si}_n\text{O}_m$  ( $n = 1, 2; m = 1-4$ ) clusters are all planar structures. The most stable structures of  $\text{Si}_n\text{S}_m$  ( $n = 1, 2; m = 1-4$ ) clusters are similar to those of  $\text{Si}_n\text{O}_m$  except that  $\text{Si}_2\text{S}_2$  has a bent non-planar structure which is slightly different from the planar rhombus of  $\text{Si}_2\text{O}_2$ . Maity *et al.*<sup>52</sup> predicted that the most stable structures of  $\text{CS}_3$  and  $\text{CS}_4$  clusters are both  $C_{2v}$  symmetric planar structures. The most stable structures of  $\text{SiS}_3$  and  $\text{SiS}_4$  in this work are similar to those of  $\text{CS}_3$  and  $\text{CS}_4$ . However, the structures of  $\text{Si}_2\text{S}$  and  $\text{Si}_2\text{S}_2$  are very different from those of  $\text{C}_2\text{S}$  and  $\text{C}_2\text{S}_2$ . The most stable structures of  $\text{C}_2\text{S}$ <sup>55</sup> is found to be linear with the S atom attaching to one end of C=C bond and that of  $\text{C}_2\text{S}_2$  is also linear with the S atoms attaching to two ends of C=C bond.<sup>56</sup> In this work, the most stable structures of  $\text{Si}_2\text{S}$  and  $\text{Si}_2\text{S}_2$  are both cyclic structures instead of linear structures. The structural differences between  $\text{Si}_2\text{S}_m$  and  $\text{C}_2\text{S}_m$  ( $m = 1, 2$ ) probably are because the two carbon atoms prefer to form bonds with each other via  $sp^2$  hybridization while the silicon atoms prefer  $sp^3$  hybridization.

#### IV. CONCLUSIONS

$\text{Si}_n\text{S}_m^-$  ( $n = 1, 2; m = 1-4$ ) cluster anions were investigated with photoelectron spectroscopy. The structures of these cluster anions and their corresponding neutrals were also studied by *ab initio* calculations. The most probable structures of the  $\text{Si}_n\text{S}_m^-$  clusters were determined by comparing the calculated VDEs to the experimental results. We found that the most stable isomers of the  $\text{Si}_n\text{S}_m^-$  ( $n = 1, 2; m = 1-4$ ) clusters prefer to adopt planar structures except that  $\text{Si}_2\text{S}_4^-$  has a non-planar structure with one S atom bent out of the plane. The neutral  $\text{Si}_n\text{S}_m$  ( $n = 1, 2; m = 1-4$ ) clusters also prefer to adopt planar structures except that the structure of  $\text{Si}_2\text{S}_2$  is slightly bent. The Si atom is inclined to interact with more S atoms.

#### ACKNOWLEDGMENTS

This work is supported by the Natural Science Foundation of China (Grant No. 21303214) and the Knowledge Innovation Program of the Chinese Academy of Sciences (Grant No. KJCX2-EW-H01). The theoretical calculations were conducted on the ScGrid and DeepComp 7000 of the Supercomputing Center, Computer Network Information Center of the Chinese Academy of Sciences. We are grateful to Professor Ralf I. Kaiser for valuable discussion.

- <sup>1</sup>M. K. Weldon, K. T. Queeney, J. Eng, Jr., K. Raghavachari, and Y. J. Chabal, *Surf. Sci.* **500**, 859 (2002).
- <sup>2</sup>I. Žutić, J. Fabian, and S. D. Sarma, *Rev. Mod. Phys.* **76**, 323 (2004).
- <sup>3</sup>K. Willacy and I. Cherchneff, *Astron. Astrophys.* **330**, 676 (1998).
- <sup>4</sup>R. Mauersberger, U. Ott, C. Henkel, J. Cernicharo, and R. Gallino, *Astron. Astrophys.* **426**, 219 (2004).
- <sup>5</sup>S. Daflon, K. Cunha, R. de la Reza, J. Holtzman, and C. Chiappini, in *Chemical Abundances in the Universe: Connecting First Stars to Planets*, edited by K. Cunha, M. Spite, and B. Barbuy (Cambridge University Press, Cambridge, 2010), pp. 358.
- <sup>6</sup>N. Dauphas, *Nature* **501**, 175 (2013).
- <sup>7</sup>H. B. Franz, S. T. Kim, J. Farquhar, J. M. Day, R. C. Economos, K. D. McKeegan, A. K. Schmitt, A. J. Irving, J. Hoek, and J. Dottin, *Nature* **508**, 364 (2014).
- <sup>8</sup>S. Klinge, J. Hirst, J. D. Maman, T. Krude, and L. Pellegrini, *Nat. Struct. Mol. Biol.* **14**, 875 (2007).
- <sup>9</sup>G. Andre, S. Even, H. Putzer, P. Burguiere, C. Croux, A. Danchin, I. MartinVerstraete, and O. Soutourina, *Nucleic Acids Res.* **36**, 5955 (2008).
- <sup>10</sup>T. N. Kitsopoulos, C. J. Chick, A. Weaver, and D. M. Neumark, *J. Chem. Phys.* **93**, 6108 (1990).
- <sup>11</sup>T. N. Kitsopoulos, C. J. Chick, Y. Zhao, and D. M. Neumark, *J. Chem. Phys.* **95**, 1441 (1991).
- <sup>12</sup>C. Heinemann, W. Koch, G. G. Lindner, and D. Reinen, *Phys. Rev. A* **52**, 1024 (1995).
- <sup>13</sup>S. Hunsicker, R. O. Jones, and G. Gantefor, *J. Chem. Phys.* **102**, 5917 (1995).
- <sup>14</sup>C. Xu, T. R. Taylor, G. R. Burton, and D. M. Neumark, *J. Chem. Phys.* **108**, 1395 (1998).
- <sup>15</sup>M. D. Chen, M. L. Liu, L. S. Zheng, Q. E. Zhang, and C. T. Au, *Chem. Phys. Lett.* **350**, 119 (2001).
- <sup>16</sup>B. X. Li, P. L. Cao, and X. Y. Zhou, *Phys. Status Solidi B* **238**, 11 (2003).
- <sup>17</sup>S. J. Peppernick, K. D. D. Gunaratne, S. G. Sayres, and A. W. Castleman, *J. Chem. Phys.* **132**, 044302 (2010).
- <sup>18</sup>J. X. Yu, X. R. Chen, and S. Sanvito, *Phys. Rev. B* **82**, 085415 (2010).
- <sup>19</sup>S. Duley, A. Chakraborty, S. Giri, and P. K. Chattaraj, *J. Sulfur Chem.* **31**, 231 (2010).
- <sup>20</sup>M. Haertelt, J. T. Lyon, P. Claes, J. de Haeck, P. Lievens, and A. Fielicke, *J. Chem. Phys.* **136**, 064301 (2012).
- <sup>21</sup>J. B. Kim, C. Hock, T. I. Yacovitch, and D. M. Neumark, *J. Phys. Chem. A* **117**, 8126 (2013).
- <sup>22</sup>D. A. Haas, *Angew. Chem. Int. Ed.* **4**, 1014 (1965).
- <sup>23</sup>R. D. Davy and S. Holiday, *Chem. Phys. Lett.* **232**, 313 (1995).
- <sup>24</sup>R. D. Davy and H. F. Schaefer, *Chem. Phys. Lett.* **255**, 171 (1996).
- <sup>25</sup>Z. Y. Liu, R. B. Huang, and L. S. Zheng, *Int. J. Mass Spectrom. Ion Processes* **155**, 79 (1996).
- <sup>26</sup>S. F. Wang, J. K. Feng, K. Q. Yu, M. Cui, A. M. Ren, C. C. Sun, P. Liu, Z. Gao, and F. A. Kong, *J. Mol. Struct. THEOCHEM* **499**, 241 (2000).
- <sup>27</sup>S. F. Wang, J. K. Feng, C. C. Sun, P. Liu, Z. Gao, and F. A. Kong, *Int. J. Quantum Chem.* **81**, 280 (2001).
- <sup>28</sup>S. F. Wang, J. K. Feng, C. C. Sun, P. Liu, Z. Gao, and F. A. Kong, *Theor. Chem. Acc.* **106**, 163 (2001).
- <sup>29</sup>M. A. Zwijnenburg, R. G. Bell, and F. Corà, *J. Solid State Chem.* **181**, 2480 (2008).
- <sup>30</sup>M. Morris, W. Gilmore, P. Palmer, B. E. Turner, and B. Zuckerman, *Astrophys. J.* **199**, L47 (1975).
- <sup>31</sup>M. C. McCarthy, C. A. Gottlieb, P. Thaddeus, S. Thorwirth, and J. Gauss, *J. Chem. Phys.* **134**, 034306 (2011).
- <sup>32</sup>L. A. Muck, V. Lattanzi, S. Thorwirth, M. C. McCarthy, and J. Gauss, *Angew. Chem. Int. Ed.* **51**, 3695 (2012).
- <sup>33</sup>H.-G. Xu, Z.-G. Zhang, Y. Feng, J. Y. Yuan, Y. C. Zhao, and W. J. Zheng, *Chem. Phys. Lett.* **487**, 204 (2010).
- <sup>34</sup>C. Lee, W. Yang, and R. G. Parr, *Phys. Rev. B* **37**, 785 (1988).
- <sup>35</sup>A. D. Becke, *J. Chem. Phys.* **98**, 5648 (1993).
- <sup>36</sup>T. H. Dunning, *J. Chem. Phys.* **90**, 1007 (1989).
- <sup>37</sup>J. A. Pople, M. Head-Gordon, and K. Raghavachari, *J. Chem. Phys.* **87**, 5968 (1987).
- <sup>38</sup>M. J. Frisch, G. W. Trucks, H. B. Schlegel *et al.*, Gaussian 09, Revision A.02, Gaussian, Inc., Wallingford, CT, 2009.
- <sup>39</sup>S. M. Harris, R. A. Gottscho, R. W. Field, and R. F. Brarrow, *J. Mol. Spectrosc.* **91**, 35 (1982).
- <sup>40</sup>See supplementary material at <http://dx.doi.org/10.1063/1.4896384> for the photoelectron spectra of  $\text{Si}_2\text{S}_m^-$  ( $m = 1 = 3$ ) taken with 532 nm, the Cartesian coordinates of the stable isomers of  $\text{Si}_n\text{S}_m^-$  clusters, and the vibrational frequencies, infrared intensities, dipole moments, and rotational constants of the most stable  $\text{Si}_n\text{S}_m$  neutral clusters.
- <sup>41</sup>D. J. Tozer and N. C. Handy, *J. Chem. Phys.* **109**, 10180 (1998).
- <sup>42</sup>J. Akola, M. Manninen, H. Häkkinen, U. Landman, X. Li, and L.-S. Wang, *Phys. Rev. B* **60**, R11297 (1999).
- <sup>43</sup>A. I. Boldyrev and J. Simons, *J. Phys. Chem.* **97**, 5875 (1993).
- <sup>44</sup>V. A. Mozhayskiy and A. Krylov, ezSpectrum, see <http://iopopshell.usc.edu/downloads>.
- <sup>45</sup>L. S. Wang, S. R. Desai, H. Wu, and J. B. Nicholas, *Z. Phys. D* **40**, 36 (1997).
- <sup>46</sup>A. D. Walsh, *J. Chem. Soc.* 2266 (1953).
- <sup>47</sup>L. S. Wang, H. B. Wu, S. R. Desai, J. W. Fan, and S. D. Colson, *J. Phys. Chem.* **100**, 8697 (1996).
- <sup>48</sup>L. S. Wang, J. B. Nicholas, M. Dupuis, H. B. Wu, and S. D. Colson, *Phys. Rev. Lett.* **78**, 4450 (1997).
- <sup>49</sup>W. C. Lu, C. Z. Wang, V. Nguyen, M. W. Schmidt, M. S. Gordon, and K. M. Ho, *J. Phys. Chem. A* **107**, 6936 (2003).
- <sup>50</sup>K. Sen, D. Ghosh, S. Pakhira, T. Banu, and A. K. Das, *J. Chem. Phys.* **139**, 234303 (2013).
- <sup>51</sup>H. B. Du, S. P. Huang, A. De Sarkar, W. J. Fan, Y. Jia, and R. Q. Zhang, *J. Phys. Chem. A* (published online).
- <sup>52</sup>S. Maity, Y. S. Kim, R. I. Kaiser, H. M. Lin, B. J. Sun, and A. H. H. Chang, *Chem. Phys. Lett.* **577**, 42 (2013).
- <sup>53</sup>H. Wang, J. Szczepanski, P. Brucat, and M. Vala, *Int. J. Quantum Chem.* **102**, 795 (2005).
- <sup>54</sup>G. Pascoli and H. Lavendy, *Int. J. Mass Spectrom.* **181**, 11 (1998).
- <sup>55</sup>I. Perez-Juste, A. M. Grana, L. Carballeira, and R. A. Mosquera, *J. Chem. Phys.* **121**, 10447 (2004).
- <sup>56</sup>K.-H. Kim, B. Lee, and S. Lee, *Chem. Phys. Lett.* **297**, 65 (1998).
- <sup>57</sup>G. P. Raine, H. F. Schaefer III, and R. C. Haddon, *J. Am. Chem. Soc.* **105**, 194 (1983).